

---

# Calibrated Reliable Regression using Maximum Mean Discrepancy

---

Peng Cui<sup>1,2</sup>, Wenbo Hu<sup>1,2</sup>, Jun Zhu<sup>1\*</sup>

<sup>1</sup> Dept. of Comp. Sci. & Tech., Institute for AI, BNRist Center  
Tsinghua-Bosch Joint ML Center, THBI Lab, Tsinghua University, Beijing, 100084 China

<sup>2</sup> RealAI

xpeng.cui@gmail.com, wenbo.hu@realai.ai, dcszj@tsinghua.edu.cn

## Abstract

Accurate quantification of uncertainty is crucial for real-world applications of machine learning. However, modern deep neural networks still produce unreliable predictive uncertainty, often yielding over-confident predictions. In this paper, we are concerned with getting well-calibrated predictions in regression tasks. We propose the calibrated regression method using the maximum mean discrepancy by minimizing the kernel embedding measure. Theoretically, the calibration error of our method asymptotically converges to zero when the sample size is large enough. Experiments on non-trivial real datasets show that our method can produce well-calibrated and sharp prediction intervals, which outperforms the related state-of-the-art methods.

## 1 Introduction

Deep learning has achieved significant progress on a wide range of complex tasks [22] mainly in terms of some metrics on prediction accuracy. However, high accuracy alone is often not sufficient to characterize the performance in real applications, where uncertainty is pervasive because of various facts such as incomplete knowledge, ambiguities, and contradictions. Accurate quantification of uncertainty is crucial to derive a robust prediction rule. For example, an accurate uncertainty estimate can reduce the occurrence of accidents in medical diagnosis [23], warn users in time in self-driving systems [27], reject low-confidence predictions [6], and better meet consumers' order needs of internet services especially on special events [39]. In general, there are two main types of uncertainty, *aleatoric* uncertainty and *epistemic* uncertainty [10]. *Aleatoric* uncertainty captures inherent data noise (e.g., sensor noise), while *epistemic* uncertainty is considered to be caused by model parameters and structure, which can be reduced by providing enough data.

Though important, it is highly nontrivial to properly characterize uncertainty. Deep neural networks (DNNs) typically produce point estimates of parameters and predictions, and are insufficient to characterize uncertainty because of their deterministic functions [11]. It has been widely observed that the modern neural networks are not properly calibrated and often tend to produce over-confident predictions [3, 15]. An effective uncertainty estimation is to directly model the predictive distribution with the observed data in a Bayesian style [26]. But performing Bayesian inference on deep networks is still a very challenging task, where the networks define highly nonlinear functions and are often over-parameterized [34, 38]. The uncertainty estimates of Bayesian neural networks (BNNs) may lead to an inaccurate uncertainty quantification because of either model misspecification or the use of approximate inference [19]. Besides, BNNs are computationally more expensive and slower to train in practice, compared to non-Bayesian NNs. For example, a simple method of MC-Dropout directly

---

\*J.Z is the corresponding author.

captures uncertainty without changing the network structure [12]. But the uncertainty quantification of MC-Dropout can be inaccurate, as will be seen in the empirical results in this paper.

Apart from BNNs, some methods have been developed to incorporate the variance term into NNs to estimate the predictive uncertainty. For instance, [17] proposed a heteroscedastic neural network (HNN) to combine both model uncertainty and data uncertainty simultaneously, getting the mean and variance by designing two outputs in the last layer of the network. Based on HNN, [21] described a simple and scalable method for estimating predictive uncertainty from ensembled HNNs, named as *deep ensemble*. But the ensembled model is usually computationally expensive especially when the model structure is complex.

An alternative way to obtain accurate predictive uncertainty is to calibrate the inaccurate uncertainties. Early attempts were made to use the scaling and isotonic regression techniques to calibrate the supervised learning predictions of traditional models, such as SVMs, neural networks and decision trees [29, 32]. For regression tasks, the prediction intervals are calibrated based on the proportion of covering ground truths. Recently, [15, 19] adopted a post-processing step to adjust the output probabilities of the modern neural networks based on the temperature scaling and non-parametric isotonic regression techniques. Such *post-processing* methods can be directly applied to both BNNs and DNNs without model modifications. But they need to train an auxiliary model and rely on an additional validation dataset. Moreover, the isotonic regression tends to overfit especially for small datasets [35]. [31, 36] directly incorporated a calibration error to loss functions to obtain the calibrated prediction intervals at the specific confidence level. Predetermining the specific confidence level can be regarded as the “point calibration” and its calibration model needs to be retrained when the confidence level is changed. [35] proposed an extension to the post-processing procedure of the isotonic regression, using Gaussian Processes (GPs) and Beta link functions. This method improves calibration at the distribution level compared to existing post-processing methods, but is computationally expensive because of the GPs.

In this paper, we propose a new way to obtain the calibrated predictive uncertainty of regression tasks at the global quantile level — it derives a distribution matching strategy and gets the well-calibrated distribution which can output predictive uncertainties at all confidence levels. Specifically, we minimize the maximum mean discrepancy (MMD) [13] to reduce the distance between the predicted probability uncertainty and true one. We show that the calibration error of our model asymptotically converges to zero when the sample size is sufficiently large. Extensive empirical results on the regression and time-series forecasting tasks show the effectiveness and flexibility of our method.

## 2 Preliminaries

In this section, we introduce some preliminary knowledge of calibrated regressor and maximum mean discrepancy, as well as the notations used in the sequel.

### 2.1 Calibrated Regressor

Let us denote a predictive regression model as  $f: x \rightarrow y$ , where  $x \in \mathbb{R}^d$  and  $y \in \mathbb{R}$  are random variables. We use  $\Theta$  to denote the parameters of  $f$ . We learn a proposed regression model given a labeled dataset  $\{(x_i, y_i)\}_{i=1}^N$  with  $N$  samples. To obtain more detailed uncertainty of the output distribution, a calibrated regressor outputs the cumulative distribution function (CDF)  $F_i$  by the predictive distribution for each input  $x_i$ . When evaluating the calibration of regressors, the inverse function of CDF  $F_i^{-1}: [0, 1] \rightarrow \hat{y}_i$  is used to denote the quantile function:

$$F_i^{-1}(p) = \inf \{y : p \leq F_i(y)\}. \quad (1)$$

Intuitively, the calibrated regressor should produce calibrated prediction intervals (PIs). For example, given the probability 95%, the calibrated regressor should output the prediction interval that approximately covers 95% of ground truths in the long run.

Formally, we define a *well-calibrated* regressor [8, 19] if the following condition holds, for all  $p \in [0, 1]$ ,

$$\frac{\sum_{i=1}^N \mathbb{I}\{y_i \leq F_i^{-1}(p)\}}{N} \rightarrow p, \text{ when } N \rightarrow \infty, \quad (2)$$

where  $\mathbb{I}(\cdot)$  is the indicator function that equals to 1 if the predicate holds otherwise 0. More generally, for a prediction interval  $[F_i^{-1}(p_1), F_i^{-1}(p_2)]$ , there is a similar definition of two-sided calibration as follows:

$$\frac{\sum_{i=1}^N \mathbb{I}\{F_i^{-1}(p_1) \leq y_i \leq F_i^{-1}(p_2)\}}{N} \rightarrow p_2 - p_1 \quad \text{for all } p_1, p_2 \in [0, 1] \quad (3)$$

as  $N \rightarrow \infty$ .

For this task, the previous methods applied the post-processing techniques [15, 19] or added a regularized loss [31, 36]. But when we want to get PIs with different confidence levels, we need to retrain the model because the confidence level is predetermined in the loss function. In contrast, we argue that the key challenge for the calibrated regression is getting the well-calibrated distribution. Based on this principle, our method utilizes the distribution matching strategy and aims to directly get a calibrated predictive distribution, which can naturally output well-calibrated CDF and PIs for each input  $x_i$ .

## 2.2 Maximum Mean Discrepancy

Our method adopts maximum mean discrepancy (MMD) to perform distribution matching. Specifically, MMD is defined via the Hilbert space embedding of distributions, known as kernel mean embedding [13]. Formally, given a probability distribution, the kernel mean embedding represents it as an element in a reproducing kernel Hilbert space (RKHS). An RKHS  $\mathcal{F}$  on  $\mathcal{X}$  with the kernel function  $k$  is a Hilbert space of functions  $g : \mathcal{X} \rightarrow \mathbb{R}$ . We use  $\phi(x) = k(x, \cdot)$  to represent the feature map of  $x$ . The expectation of embedding on its feature map is defined as:

$$\mu_X := \mathbb{E}_X[\phi(X)] = \int_{\Omega} \phi(x)P(dx). \quad (4)$$

This kernel mean embedding can be used for density estimation and two-sample test [13].

Based on the Hilbert space embedding, the maximum mean discrepancy (MMD) estimator was developed to distinguish two distributions  $P$  and  $Q$  [13]. Formally, the MMD measure is defined as follows:

$$L_m(P, Q) = \|\mathbb{E}_X(\phi(P)) - \mathbb{E}_X(\phi(Q))\|_{\mathcal{F}}. \quad (5)$$

The MMD estimator is guaranteed to be unbiased and has nearly minimal variance among unbiased estimators [25]. Moreover, it was shown that  $L_m(P, Q) = 0$  if and only if  $P = Q$  [13].

We conduct a hypothesis test with null hypotheses  $H_0 : P = Q$ , and the alternative hypotheses  $H_1 : P \neq Q$  if  $L_m(P, Q) > c_\alpha$  for some chosen threshold  $c_\alpha > 0$ . With a characteristic kernel function (e.g., the popular RBF kernels), the MMD measure can be used to distinguish the two different distributions and have been applied to generative modeling [24, 25].

In practice, the MMD objective can be estimated using the empirical kernel mean embeddings:

$$\hat{L}_m^2(P, Q) = \left\| \frac{1}{N} \sum_{i=1}^N \phi(x_{1i}) - \frac{1}{M} \sum_{j=1}^M \phi(x_{2j}) \right\|_{\mathcal{F}}^2, \quad (6)$$

where  $x_{1i}$  and  $x_{2j}$  are independent random samples drawn from the distributions  $P$  and  $Q$  respectively.

## 3 Calibrated Regression with Maximum Mean Discrepancy

We now present the uncertainty calibration with the maximum mean discrepancy and then plug it into the proposed calibrated regression model. We also give the theoretical guarantee to show the effectiveness of our uncertainty calibration strategy.

### 3.1 Uncertainty Calibration with Distribution Matching

Specifically in this part, we use  $P$  and  $Q$  to represent the unknown true distribution and predictive distribution of our regression model respectively. The distribution matching strategy of our uncertainty

calibration model is to directly minimize the kernel embedding measure defined by MMD in Eqn. (6). The specific goal is to let the predictive distribution  $Q$  converge asymptotically to the unknown target distribution  $P$  so that we can get the calibrated CDFs  $\{F_i\}$ . The strategy is to minimize the MMD distance measure between the regression ground-truth targets  $\{y_1, \dots, y_n\}$  and random samples  $\{\hat{y}_1, \dots, \hat{y}_n\}$  from the predictive distribution  $Q$ . The specific form of the MMD distance loss  $L_m$  is:

$$L_m^2(P, Q) := \left\| \frac{1}{N} \sum_{i=1}^N \phi(y_i) - \frac{1}{N} \sum_{j=1}^N \phi(\hat{y}_j) \right\|_{\mathcal{F}}^2. \quad (7)$$

We use a mixture of  $k$  kernels spanning multiple ranges for our experiments:

$$k(x, x') = \sum_{i=1}^K k_{\sigma_i}(x, x'), \quad (8)$$

where  $k_{\sigma_i}$  is an RBF kernel and the bandwidth parameter  $\sigma_i$  can be chosen simple values such as 2,4,8, etc. The kernel was proved to be characteristic, and it can maximize the two-sample test power and low test error [14]. In general, a mixture of five kernels or more is sufficient to obtain good results.

With the incorporation of this MMD loss, we learn the calibrated predictive probability distribution and the obtained uncertainties can be generalized to arbitrary confidence levels without retraining.

In theory, under  $H_0 : P = Q$ , the predictive distribution  $Q$  will converge asymptotically to the true distribution  $P$  as sample size  $N \rightarrow \infty$ , which is why minimizing MMD loss is effective for uncertainty calibration. Leveraging our distribution matching strategy, the uncertainty calibration can be achieved by narrowing the gap between  $P$  and  $Q$ . Formally, we have the following theoretical result:

**Theorem 1.** *Suppose that the predictive distribution  $Q$  has the sufficient ability to approximate the true unknown distribution  $P$ , given data is i.i.d. Eqn. (9) holds by minimizing the MMD loss  $L_m = \|\mu_{x_1} - \mu_{x_2}\|_{\mathcal{F}}$  in our proposed methodology as the sample size  $N \rightarrow \infty$*

$$\frac{\sum_{i=1}^N \mathbb{I}\{y_i \leq F_i^{-1}(p)\}}{N} \rightarrow p \quad \text{for all } p \in [0, 1] \quad (9)$$

*Proof.*  $L_m(P, Q) = 0$  if and only if  $P = Q$  when  $\mathcal{F}$  is a unit ball in a universal RKHS [13]. Under  $H_0 : P = Q$ , the predictive distribution  $Q(x)$  will converge asymptotically to the unknown true distribution  $P(x)$  as the sample size  $N \rightarrow \infty$  by minimizing the MMD loss  $L_m$ . Further, Eqn. (9) holds according to the obtained predictive distribution. Because the confidence level  $p$  is exactly equal to the proportion of samples  $\{y_1, \dots, y_n\}$  covered by the prediction interval.  $\square$

This theoretical result can be generalized to the two side calibration condition defined in Eqn. (3) and we defer the details to Appendix A.

### 3.2 Calibrated Regression with MMD

To represent the model uncertainty, we use a heteroscedastic neural network (HNN) to get the predictive distribution and outputs the predicted mean  $\mu(x)$  and the variance  $\sigma^2(x)$  in the final layer, which can combine epistemic uncertainty and aleatoric uncertainty in one model [17, 30].

Based on this representation model, we use a two-stage learning framework which optimizes the two objectives one by one, namely the negative log likelihood loss  $L_h$  and the uncertainty calibration loss  $L_m$ . In the first stage, the optimal model parameters can be learned by minimizing negative log-likelihood loss (NLL):

$$L_h(\Theta) = \sum_{i=1}^N \frac{\log \sigma_{\Theta}^2(x_i)}{2} + \frac{(y_i - \mu_{\Theta}(x_i))^2}{2\sigma_{\Theta}^2(x_i)} + \text{constant}. \quad (10)$$

In practice, to improve numerical stability, we optimize the following equivalent form:

$$L_h(\Theta) = \sum_{i=1}^N \frac{1}{2} \exp(-s_i) (y_i - \mu_{\Theta}(x_i))^2 + \frac{1}{2} s_i, \quad s_i := \log \sigma_{\Theta}^2(x_i). \quad (11)$$

Although the Gaussian assumption is a bit restrictive above, we found that the method performs satisfactorily well in our experiments. In the second stage, we minimize the uncertainty calibration loss with MMD, i.e., Eqn. (7).

The overall procedure is two-stage:

$$\begin{aligned} \text{step 1:} & \quad \min_{\Theta} L_h(\Theta; y, f(x)), \\ \text{step 2:} & \quad \min_{\Theta} L_m(\Theta; y, f(x)), \end{aligned} \tag{12}$$

where  $L_m$  is the loss function of distribution matching objective, and  $L_h$  is the loss function of distribution estimation. We detail the whole process of the framework in Algorithm 1. The main merits of the two-stage learning are to 1) utilize the representation capability of the HNN model in the first stage and 2) learn the calibrated predictive distribution via the distribution matching strategy in the second stage. Compared with the bi-level learning algorithm used in [19] which iterates the two stages for several times, our method runs with one time iteration of the two stages, which reduces the computation cost of the kernel-based MMD component.

**Comparison with Post-processing Calibration Methods** The previous post-processing methods [19, 31, 36] calibrate the uncertainty outputs of the input dataset without any model modifications and needs to be retrained when the confidence level is changed. In contrast, the proposed distribution matching with MMD, albeit also regarded as a post-processing procedure, learns the calibrated predictive model, which means practitioners are not required to retrain the model but can enjoy the calibration performance.

---

**Algorithm 1** Deep calibrated reliable regression model.

---

**Input:**

Labeled training data and kernel bandwidth parameters

**Output:**

Trained mean  $\mu(x_i)$  and variance  $\sigma(x_i)$  for the predictive distribution

- 1: **while** not converged **do**
  - 2:   Compute  $\mu(x_i)$  and  $\log \sigma(x_i)$
  - 3:   Compute NLL loss  $L_h$  by Eqn. (11)
  - 4:   Update model parameters  $\Theta = \arg \min_{\Theta} L_h(\Theta; y, f(x))$  by SGD
  - 5: **end while**
  - 6: **while** not converged **do**
  - 7:   Compute  $\mu(x_i)$  and  $\log \sigma(x_i)$ , randomly sampling data  $\{\hat{y}_i\}_{i=1}^N$  from predictive distribution
  - 8:   Compute MMD loss  $L_m$  by Eqn. (7)
  - 9:   Update model parameters  $\Theta = \arg \min_{\Theta} L_m(\Theta; y, f(x))$  by SGD
  - 10: **end while**
  - 11: **return** a trained model  $f(x)$ ;
- 

## 4 Experiments

In this section, we compare the proposed method with several strong baselines on the regression and time-series forecasting tasks in terms of predictive uncertainty. The time-series forecasting task models multiple regression sub-problems in sequence and the tendency along the sliding windows can be used to examine the obtained predictive uncertainty. Then we show the sensitivity analysis and the time efficiency of our proposed method.

### 4.1 Datasets and Experimental Settings

**Baselines** We compare with several competitive baselines, including MC-Dropout (MCD) [12], Heteroscedastic Neural Network (HNN) [17], Deep Ensembles (Deep-ens) [21], Ensembled Likelihood (ELL), MC-Dropout Likelihood (MC NLL), Deep Gaussian Processes (DGP) [33] and the post-hoc calibration method using isotonic regression (ISR) [19]. ELL and MC NLL are our proposed variants inspired by Deep Ensemble. The variance of ELL is computed by predictions from multiple networks during the training phase, and the variance of MC NLL is computed by multiple random predictions based on MC-Dropout during the training phase. Details of these compared methods can be found in Appendix B.1.

**Hyperparameters** For all experimental results, we report the averaged results and std. errors obtained from 5 random trials. The details of hyperparameters setting can be found in Appendix B.2.

**Datasets** We use several public datasets from UCI repository [2] and Kaggle [1]: 1) for the time-series task: Pickups, Bike-sharing, PM2.5, Metro-traffic and Quality; 2) for the regression task: Power Plant, Protein Structure, Naval Propulsion and wine. The details of the datasets can be found in Appendix B.3.

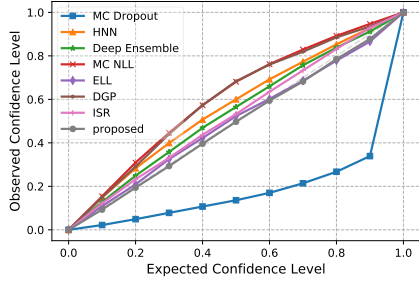
**Evaluation Metrics** We evaluate the performance using two metrics: 1) RMSE for the prediction precision; and 2) the calibration error. The calibration error is the absolute difference between true confidence and empirical coverage probability. We use two variants: the expectation of coverage probability error (ECPE) and the maximum value of coverage probability error (MCPE). We put the detailed definitions of the metrics in Appendix C.

## 4.2 Results of Time-series Forecasting Tasks

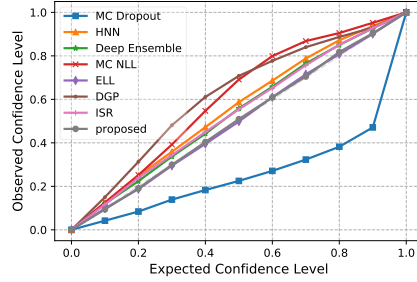
For time-series forecasting tasks, we construct an LSTM model with two hidden layers (128 hidden units and 64 units respectively) and a linear layer for making the final predictions. The size of the sliding window is 5 and the forecasting horizon is 1. Take the Bike-sharing dataset as an example, the bike sharing data of the past five hours will be used to predict the data of one hour in the future. All datasets are split into 70% training data and 30% test data.

Dataset	Metric	MCD	HNN	Deep-ens	MC NLL
Metro-traffic	ECPE	0.304±0.005	0.102±0.002	0.100±0.001	0.142±0.010
	MCPE	0.505±0.011	0.162±0.003	0.160±0.002	0.235±0.014
	RMSE	523.6±6.725	556.3±3.332	<b>508.9±1.288</b>	631.6±14.23
Bike-sharing	ECPE	0.258±0.011	0.054±0.002	0.038±0.001	0.119±0.013
	MCPE	0.432±0.020	0.089±0.004	0.066±0.008	0.206±0.022
	RMSE	38.86±0.141	40.71±0.542	<b>37.60±0.355</b>	61.57±1.624
Pickups	ECPE	0.246±0.017	0.078±0.001	0.064±0.006	0.088±0.016
	MCPE	0.408±0.025	0.117±0.005	0.098±0.011	0.136±0.010
	RMSE	350.3±6.562	359.8±3.421	336.4±1.653	526.8±9.214
PM2.5	ECPE	0.331±0.013	0.022±0.001	0.026±0.003	0.081±0.010
	MCPE	0.550±0.025	0.050±0.004	0.060±0.004	0.151±0.027
	RMSE	70.95±2.629	58.81±0.372	60.24±0.114	66.77±3.613
Air-quality	ECPE	0.329±0.005	0.058±0.003	0.045±0.001	0.111±0.004
	MCPE	0.561±0.008	0.091±0.006	0.072±0.002	0.178±0.004
	RMSE	81.16±0.111	<b>79.60±0.254</b>	80.03±0.236	87.12±0.971
Dataset	Metric	ELL	DGP	ISR	proposed
Metro-traffic	ECPE	0.048±0.017	0.115±0.007	0.032±0.002	<b>0.017±0.001</b>
	MCPE	0.075±0.027	0.192±0.013	0.051±0.003	<b>0.036±0.002</b>
	RMSE	613.5±18.63	646.4±0.302	556.3±3.332	545.5±4.225
Bike-sharing	ECPE	0.027±0.003	0.121±0.003	0.042±0.002	<b>0.006±0.001</b>
	MCPE	0.048±0.055	0.213±0.005	0.066±0.005	<b>0.019±0.002</b>
	RMSE	52.50±2.901	55.39±0.397	40.71±0.542	37.93±0.334
Pickups	ECPE	0.018±0.008	0.098±0.003	0.049±0.002	<b>0.008±0.001</b>
	MCPE	0.038±0.016	0.160±0.005	0.075±0.004	<b>0.023±0.001</b>
	RMSE	<b>325.9±11.23</b>	440.3±3.469	359.8±3.421	346.9±4.652
PM2.5	ECPE	0.080±0.007	0.061±0.006	0.023±0.002	<b>0.010±0.000</b>
	MCPE	0.119±0.011	0.149±0.014	0.057±0.006	<b>0.035±0.003</b>
	RMSE	61.09±0.434	61.44±2.113	58.81±0.372	<b>57.43±0.332</b>
Air-quality	ECPE	0.018±0.005	0.102±0.002	0.030±0.001	<b>0.010±0.001</b>
	MCPE	0.04±0.008	0.181±0.003	0.044±0.005	<b>0.026±0.001</b>
	RMSE	90.01±0.566	86.05±0.210	79.60±0.254	80.69±0.292

Table 1: The forecast and calibration error scores of each method on different datasets. Each row corresponds to the results of a specific method in a particular metric.

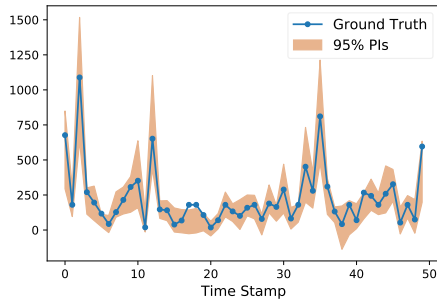


(a) Dataset: Air Quality.

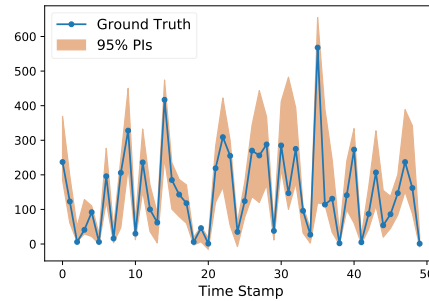


(b) Dataset: Bike Sharing.

Figure 1: For the time-series forecasting task, we plot the expected confidence vs observed confidence for all methods. The closer to the diagonal line, the uncertainty calibration is better. The results of other datasets can be found in Appendix.



(a) Dataset: Air Quality.



(b) Dataset: Bike Sharing.

Figure 2: Calibrated forecasting: Displayed prediction intervals (PIs) obtained at the 95% confidence level by our proposed method in a time-series. As shown in the figure, the prediction intervals are also sharp while accurately covering the ground truth. The results of other datasets can be found in Appendix.

Table 1 present the results of all the methods, including the forecast and calibration errors. We can see that our method with the MMD distribution matching strategy achieves the accurate forecasting results on par with the strong baselines in terms of RMSE<sup>2</sup>, but significantly outperforms the baselines in the uncertainty calibration, in terms of ECPE and MCPE on all data-sets. Besides, we prefer prediction intervals as tight as possible while accurately covering the ground truth in regression tasks. We measure the sharpness using the width of prediction intervals, which is detailed in Appendix C. And our method also gets a relatively tighter prediction interval through the reported calibration sharpness from Table 4 in the Appendix. In addition, the ensemble method is second only to ours, due to the powerful ability of the ensemble of multiple networks. But when the network complexity is greater than the data complexity, the computation of the ensemble method is quite expensive, while our method can also be applied to more complex NNs. Figure 1 shows the proportion that PIs covering ground truths at different confidence levels. The result of our model is closest to the diagonal line, which indicates the best uncertainty calibration among all methods. Figure 2 shows the predictions and corresponding 95% prediction intervals. The intervals are visually sharp and accurately cover the ground truths.

### 4.3 Results of Regression Tasks

For regression tasks, we used a fully connected neural network with two hidden layers (256 hidden units) and each layer has a ReLU activation function. The size of our networks is close to the previous works [12, 19, 21] on regression problems. We evaluate on four UCI datasets varying in size from 4,898 to 45,730 samples. We randomly split 80% of each data-set for training and the rest for testing. Table 2 presents the results of all methods, where we can draw similar conclusions as in the time-series forecasting tasks. The forecast results of our method is competitive in terms of RMSE and the calibration error of our method is significantly smaller than existing methods. Figure

<sup>2</sup>In Table 5 in the Appendix, we also show the results in other metrics, such as  $R^2$ , SMAPE, etc., which have a similar conclusion.

3 reflects that the uncertainty calibration performance of each method at different confidence levels in general regression tasks and we find that our method significantly improves calibration.

Dataset	Metric	MCD	HNN	Deep-ens	MC NLL
Power Plant	ECPE	0.235±0.021	0.094±0.002	0.084±0.004	0.095±0.004
	MCPE	0.386±0.038	0.151±0.007	0.142±0.001	0.153±0.004
	RMSE	<b>3.792±0.171</b>	3.843±0.165	3.945±0.150	3.936±0.158
Protein Structure	ECPE	0.365±0.011	0.042±0.006	0.049±0.001	0.086±0.005
	MCPE	0.635±0.021	0.071±0.005	0.084±0.002	0.138±0.005
	RMSE	<b>4.088±0.014</b>	4.337±0.021	4.255±0.010	4.574±0.018
Naval Propulsion	ECPE	0.175±0.077	0.038±0.006	0.270±0.016	0.216±0.042
	MCPE	0.283±0.116	0.065±0.007	0.431±0.025	0.344±0.047
	RMSE	0.001±0.000	0.001±0.000	0.001±0.000	0.001±0.001
Wine	ECPE	0.235±0.021	0.041±0.003	0.012±0.001	0.046±0.006
	MCPE	0.386±0.038	0.082±0.013	0.034±0.004	0.095±0.011
	RMSE	0.732±0.041	0.705±0.038	<b>0.672±0.040</b>	0.683±0.064

Dataset	Metric	ELL	DGP	ISR	proposed
Power Plant	ECPE	0.019±0.025	0.094±0.005	0.062±0.003	<b>0.007±0.001</b>
	MCPE	0.035±0.037	0.158±0.008	0.105±0.003	<b>0.024±0.003</b>
	RMSE	4.186±0.184	4.181±0.009	3.843±0.165	3.819±0.112
Protein Structure	ECPE	0.038±0.009	0.020±0.002	0.014±0.006	<b>0.006±0.000</b>
	MCPE	0.075±0.016	0.036±0.004	0.027±0.010	<b>0.024±0.002</b>
	RMSE	4.519±0.019	4.950±0.011	4.337±0.021	4.556±0.012
Naval Propulsion	ECPE	0.059±0.034	0.115±0.007	0.021±0.003	<b>0.012±0.001</b>
	MCPE	0.117±0.051	0.192±0.012	0.036±0.010	<b>0.030±0.004</b>
	RMSE	0.002±0.001	0.001±0.000	0.001±0.000	<b>0.001±0.000</b>
Wine	ECPE	0.073±0.009	0.178±0.003	0.083±0.006	<b>0.008±0.002</b>
	MCPE	0.103±0.011	0.300±0.006	0.127±0.008	<b>0.024±0.004</b>
	RMSE	0.684±0.061	0.754±0.031	0.705±0.038	0.705±0.035

Table 2: The calibration error scores of uncertainty evaluation and RMSE for each method on different datasets, each row has the results of a specific method in a particular metric. Our method improves calibration and outperforms all baselines

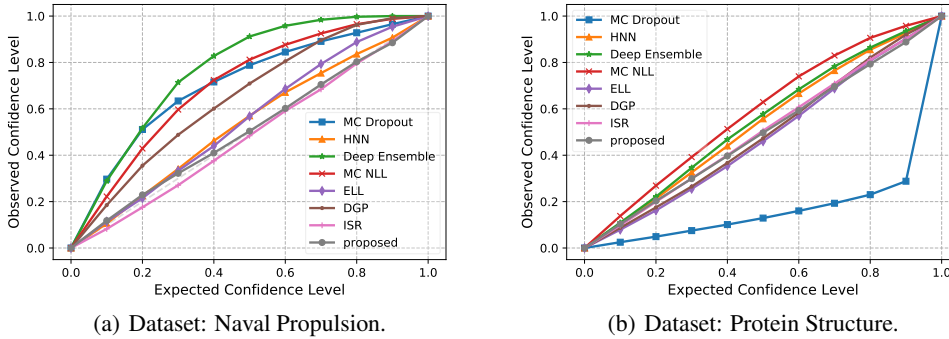


Figure 3: For the regression task, we plot the expected confidence vs observed confidence for all methods. The closer to the diagonal line, the uncertainty calibration is better. The results of other datasets can be found in Appendix.

#### 4.4 Computation Efficiency

We analyze the time complexity on the type of methods that generate the uncertainty distribution, these methods are relatively computationally expensive: DGP, Deep Ensembles, ELL and our proposed method. For the regression task, these four methods use the same network structure with a fully connected neural network (256 hidden units) at each hidden layer. The training and inference of DGP is performed using a doubly stochastic variational inference algorithm [33]. As can be seen in

Figure 4, DGP is the most time-consuming, the training time increases almost linearly as the number of network layers increases. The computation time of our method is the least among all methods when model complexity becomes higher, and can also keep low calibration error. This result coheres our argument that our method is not computationally expensive compared to the baseline methods.

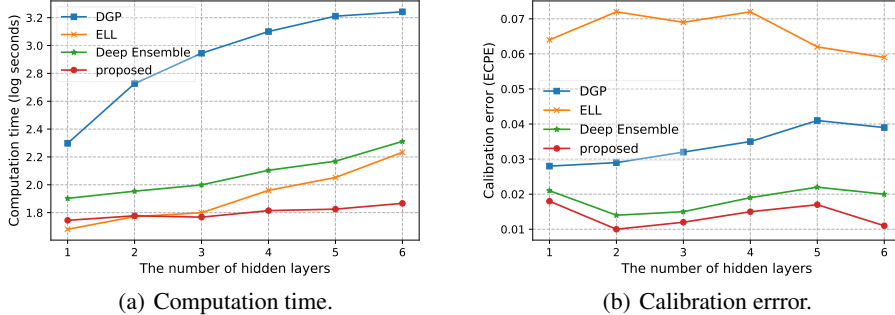


Figure 4: The computation time (log seconds) of four methods during model training phase (left) and calibration error of different models (right) on the wine dataset on GTX1080Ti. We can see that our method is also effective in computing efficiency and calibration for more complex models.

## 5 Conclusion and Discussions

We present a flexible and effective uncertainty calibration method with the MMD distribution matching strategy for regression and time-series forecasting tasks. Our method is guaranteed to produce well-calibrated predictions given sufficient data under mild assumptions. Extensive experimental results show that our method can produce reliable predictive distributions, and obtain the well-calibrated and sharp prediction intervals.

There are several directions for future investigation. Firstly, the Gaussian likelihood may be too restrictive sometimes and one could use a mixture distribution or a complex network, e.g., mixture density network [4] as a base model. Secondly, our calibration strategy can be extended to classification tasks. But the challenge we need to overcome is the impact of batch-size and binning on the performance of MMD. Thirdly, the kernels used in the MMD definition can be defined on other data structures, such as graphs and time-series [16]. Finally, it is interesting to investigate on the sample size for a given task. Specifically, we provide an asymptotic analysis on well-calibration, while in practice we only have finite data. [13] shows that MMD has performance guarantees at finite sample sizes, based on uniform convergence bounds. For our method, regardless of whether or not  $p = q$ , the empirical MMD converges in probability at rate  $O((m + n)^{-\frac{1}{2}})$  to its population value, where  $m$  and  $n$  respectively represent the number of samples sampled from  $P$  and  $Q$ . So a further investigation on the bound of our method is worth considering in the future work.

### Statement of Potential Broader Impact

Uncertainty exists in many aspects of our daily life, which plays a critical role in the application of modern machine learning methods. Unreliable uncertainty quantification may bring *safety and reliability* issues in these applications like medical diagnosis, autonomous driving, and demand forecasting. Despite deep learning has achieved impressive accuracies on many tasks, NNs are poor to provide accurate predictive uncertainty. Machine learning models should provide accurate confidence bounds (i.e., uncertainty estimation) on these safety-critical tasks.

This paper aims to solve the problem of inaccurate predictive quantification for regression models. Our method produces the well-calibrated predictive distribution while achieving the high-precision forecasting for regression tasks, and naturally generate reliable prediction intervals at any confidence level we need.

Our proposal has a positive impact on a variety of tasks using the regression models. For example, our proposed model produces more accurate demand forecasting based on the historical sales data for a retail company, which can calculate the safety stock to make sure you don't lose customers. We

believe that it is necessary to consider the uncertainty calibration for many machine learning models, which will improve the *safety and reliability* of machine learning and deep learning methods.

## Acknowledgement

We would like to thank the anonymous reviewers for their useful comments, especially for review 1 and review 3. Part of this work was done when the first two authors were working at RealAI. This work was supported by the National Key Research and Development Program of China (No.2017YFA0700904), NSFC Projects (Nos. 61620106010, U19B2034, U1811461), Beijing Academy of Artificial Intelligence (BAAI), Tsinghua-Huawei Joint Research Program, a grant from Tsinghua Institute for Guo Qiang, Tiangong Institute for Intelligent Computing, and the NVIDIA NVAIL Program with GPU/DGX Acceleration.

## References

- [1] Nyc uber pickups with weather and holidays | kaggle. <https://www.kaggle.com/yannisp/uber-pickups-enriched>. Accessed: 2020-06-04.
- [2] UCI machine learning repository. <http://archive.ics.uci.edu/ml>. Accessed: 2020-06-04.
- [3] Dario Amodei, Chris Olah, Jacob Steinhardt, Paul Christiano, John Schulman, and Dan Mané. Concrete problems in AI safety. *arXiv preprint arXiv:1606.06565*, 2016.
- [4] Christopher M Bishop. Mixture density networks. 1994.
- [5] Glenn W Brier. Verification of forecasts expressed in terms of probability. *Monthly weather review*, 78(1):1–3, 1950.
- [6] Justin Cosentino and Jun Zhu. Generative well-intentioned networks. In *Advances in Neural Information Processing Systems*, pages 13098–13109, 2019.
- [7] Andreas Damianou and Neil Lawrence. Deep Gaussian processes. In *Artificial Intelligence and Statistics*, pages 207–215, 2013.
- [8] A Philip Dawid. The well-calibrated Bayesian. *Journal of the American Statistical Association*, 77(379):605–610, 1982.
- [9] Morris H DeGroot and Stephen E Fienberg. The comparison and evaluation of forecasters. *Journal of the Royal Statistical Society: Series D (The Statistician)*, 32(1-2):12–22, 1983.
- [10] Armen Der Kiureghian and Ove Ditlevsen. Aleatory or epistemic? does it matter? *Structural safety*, 31(2):105–112, 2009.
- [11] Yarin Gal. *Uncertainty in Deep Learning*. PhD thesis, University of Cambridge, 2016.
- [12] Yarin Gal and Zoubin Ghahramani. Dropout as a Bayesian approximation: Representing model uncertainty in deep learning. In *international conference on machine learning*, pages 1050–1059, 2016.
- [13] Arthur Gretton, Karsten M Borgwardt, Malte J Rasch, Bernhard Schölkopf, and Alexander Smola. A kernel two-sample test. *Journal of Machine Learning Research*, 13(Mar):723–773, 2012.
- [14] Arthur Gretton, Dino Sejdinovic, Heiko Strathmann, Sivaraman Balakrishnan, Massimiliano Pontil, Kenji Fukumizu, and Bharath K Sriperumbudur. Optimal kernel choice for large-scale two-sample tests. In *Advances in neural information processing systems*, pages 1205–1213, 2012.
- [15] Chuan Guo, Geoff Pleiss, Yu Sun, and Kilian Q Weinberger. On calibration of modern neural networks. In *Proceedings of the 34th International Conference on Machine Learning-Volume 70*, pages 1321–1330. JMLR. org, 2017.
- [16] Thomas Hofmann, Bernhard Schölkopf, and Alexander J Smola. Kernel methods in machine learning. *The annals of statistics*, pages 1171–1220, 2008.
- [17] Alex Kendall and Yarin Gal. What uncertainties do we need in Bayesian deep learning for computer vision? *Advances in neural information processing systems*, pages 5574–5584, 2017.

- [18] Diederik P Kingma and Jimmy Ba. Adam: A method for stochastic optimization. *arXiv preprint arXiv:1412.6980*, 2014.
- [19] Volodymyr Kuleshov, Nathan Fenner, and Stefano Ermon. Accurate uncertainties for deep learning using calibrated regression. *International Conference on Machine Learning*, pages 2796–2804, 2018.
- [20] Guokun Lai, Wei-Cheng Chang, Yiming Yang, and Hanxiao Liu. Modeling long-and short-term temporal patterns with deep neural networks. In *The 41st International ACM SIGIR Conference on Research & Development in Information Retrieval*, pages 95–104, 2018.
- [21] Balaji Lakshminarayanan, Alexander Pritzel, and Charles Blundell. Simple and scalable predictive uncertainty estimation using deep ensembles. *Advances in neural information processing systems*, pages 6402–6413, 2017.
- [22] Yann LeCun, Yoshua Bengio, and Geoffrey Hinton. Deep learning. *nature*, 521(7553):436–444, 2015.
- [23] Christian Leibig, Vaneeda Allken, Murat Seçkin Ayhan, Philipp Berens, and Siegfried Wahl. Leveraging uncertainty information from deep neural networks for disease detection. *Scientific reports*, 7(1):1–14, 2017.
- [24] Chun-Liang Li, Wei-Cheng Chang, Yu Cheng, Yiming Yang, and Barnabás Póczos. MMD GAN: Towards deeper understanding of moment matching network. In *Advances in Neural Information Processing Systems*, pages 2203–2213, 2017.
- [25] Yujia Li, Kevin Swersky, and Rich Zemel. Generative moment matching networks. In *International Conference on Machine Learning*, pages 1718–1727, 2015.
- [26] David JC MacKay. A practical Bayesian framework for backpropagation networks. *Neural computation*, 4(3):448–472, 1992.
- [27] Rhiannon Michelmore, Matthew Wicker, Luca Laurenti, Luca Cardelli, Yarin Gal, and Marta Kwiatkowska. Uncertainty quantification with statistical guarantees in end-to-end autonomous driving control. In *International Conference on Robotics and Automation*, 2020.
- [28] Mahdi Pakdaman Naeini, Gregory Cooper, and Milos Hauskrecht. Obtaining well calibrated probabilities using Bayesian binning. In *Twenty-Ninth AAAI Conference on Artificial Intelligence*, 2015.
- [29] Alexandru Niculescu-Mizil and Rich Caruana. Predicting good probabilities with supervised learning. In *Proceedings of the 22nd international conference on Machine learning*, pages 625–632, 2005.
- [30] David A Nix and Andreas S Weigend. Estimating the mean and variance of the target probability distribution. In *Proceedings of 1994 IEEE international conference on neural networks (ICNN'94)*, volume 1, pages 55–60. IEEE, 1994.
- [31] Tim Pearce, Alexandra Brintrup, Mohamed Zaki, and Andy Neely. High-quality prediction intervals for deep learning: A distribution-free, ensembled approach. In *International Conference on Machine Learning*, pages 4075–4084, 2018.
- [32] John Platt et al. Probabilistic outputs for support vector machines and comparisons to regularized likelihood methods. *Advances in large margin classifiers*, 10(3):61–74, 1999.
- [33] Hugh Salimbeni and Marc Deisenroth. Doubly stochastic variational inference for deep gaussian processes. In *Advances in Neural Information Processing Systems*, pages 4588–4599, 2017.
- [34] Jiaxin Shi, Shengyang Sun, and Jun Zhu. Kernel implicit variational inference. In *International Conference on Learning Representations*, 2018.
- [35] Hao Song, Tom Diethe, Meelis Kull, and Peter Flach. Distribution calibration for regression. In *International Conference on Machine Learning*, pages 5897–5906, 2019.
- [36] Jayaraman J Thiagarajan, Bindya Venkatesh, Prasanna Sattigeri, and Peer-Timo Bremer. Building calibrated deep models via uncertainty matching with auxiliary interval predictors. In *AAAI Conference on Artificial Intelligence*, 2019.
- [37] Chris Tofallis. A better measure of relative prediction accuracy for model selection and model estimation. *Journal of the Operational Research Society*, 66(8):1352–1362, 2015.
- [38] Ziyu Wang, Tongzheng Ren, Jun Zhu, and Bo Zhang. Function space particle optimization for bayesian neural networks. In *International Conference on Learning Representations*, 2019.

- [39] Lingxue Zhu and Nikolay Laptev. Deep and confident prediction for time series at Uber. In *2017 IEEE International Conference on Data Mining Workshops (ICDMW)*, pages 103–110. IEEE, 2017.

## A Two-sided Calibration Theorem

**Theorem 2.** Suppose that the predictive distribution  $Q$  has the sufficient ability to approximate the true unknown distribution  $P$ , given data is i.i.d. Eqn. (13) holds by minimizing the MMD loss  $L_m = \|\mu_{x_1} - \mu_{x_2}\|_{\mathcal{F}}$  in our proposed methodology as the sample size  $N \rightarrow \infty$

$$\frac{\sum_{i=1}^N \mathbb{I}\{F_i^{-1}(p_1) \leq y_i \leq F_i^{-1}(p_2)\}}{N} \rightarrow p_2 - p_1 \quad \text{for all } p_1, p_2 \in [0, 1] \quad (13)$$

*Proof.*  $L_m(P, Q) = 0$  if and only if  $P = Q$  when  $\mathcal{F}$  is a unit ball in a universal RKHS [13]. Under  $H_0 : P = Q$ , the predictive distribution  $Q(x)$  will converge asymptotically to the unknown true distribution  $P(x)$  as the sample size  $N \rightarrow \infty$  by minimizing the MMD loss  $L_m$ . Further, Eqn. (13) holds according to the obtained predictive distribution. Because the confidence level  $p_2 - p_1$  is exactly equal to the proportion of samples  $\{y_1, \dots, y_n\}$  covered by the two-sided prediction interval.  $\square$

## B Experimental Setting

### B.1 Baselines

- **MC-Dropout (MCD)** [12]: A variant of standard dropout, named as Monte-Carlo Dropout. Interpreting dropout in deep neural networks as approximate Bayesian inference in deep Gaussian process. Epistemic uncertainties can be quantified with a Monte-Carlo sampling sample by using dropout during the test phase in the network without changing NNs model itself. For all experiments, the dropout probability was set at 0.3. The conventional MSE loss is used in this method.
- **Heteroscedastic Neural Network (HNN)** [17]: In this approach, similar to a heteroscedastic regression, the network has two outputs in the last layer, corresponding to the predicted mean and variance for each input  $x_i$ . HNN is trained by minimizing the negative log-likelihood loss (NLL). Epistemic uncertainty and aleatoric uncertainty can be captured by using MC-Dropout.
- **Deep Ensembles** [21]: A simple and scalable ensembled method, here referred to as Deep-ens. In this approach, predictive uncertainty is estimated by training multiple heteroscedastic neural networks independently. Each HNN is trained with the entire training dataset. In the end, the predictive distribution is considered a uniformly-weighted Gaussian mixture. For simplicity of computation, the distribution is regarded as a Gaussian for each input  $x_i$ . The mean and variance of a mixture  $M^{-1} \sum \mathcal{N}(\mu_{\Theta_m}(\mathbf{x}_i), \sigma_{\Theta_m}^2(\mathbf{x}_i))$  are given by  $\mu_*(\mathbf{x}_i) = M^{-1} \sum_m \mu_{\Theta_m}(\mathbf{x}_i)$  and  $\sigma_*^2(\mathbf{x}_i) = M^{-1} \sum_m (\sigma_{\Theta_m}^2(\mathbf{x}_i) + \mu_{\Theta_m}^2(\mathbf{x}_i)) - \mu_*^2(\mathbf{x}_i)$  respectively, where  $\{\Theta_m\}_{m=1}^M$  represent the parameters of the ensemble model. Hence the prediction intervals can be calculated by the CDF of Gaussian distribution.
- **Ensembled Likelihood (ELL)**: Inspired by deep ensemble, we jointly train  $k$  networks to minimize ensembled likelihood loss (ELL) by gradient descent algorithm, e.g. SGD. Where  $\mu_i = \frac{1}{k} \sum_{i=1}^k f_1(x_i) + f_2(x_i) + \dots + f_k(x_i)$ ,  $\sigma_i^2 = \frac{1}{k} \sum_{i=1}^k (f_i(x_i) - \mu_i)^2$ . Note that, there are interactions across these  $k$  networks, or just look at the standard deviation which is computed across predictions from different networks. This is different from typical heteroskedastic models (trained with Eqn. (14)), where the noise std.dev. comes from a single network, and it's also different from standard deep ensembles, in which you can decompose the loss across different networks (thus the networks do not interact at all during training, training networks independently). Such lack of interaction might be wasting capacity.

$$L_h(x_i, y_i) = \sum_{i=1}^N \frac{1}{2} \exp(-s_i) (y_i - \mu_{\Theta}(x_i))^2 + \frac{1}{2} s_i, \quad s_i := \log \sigma_{\Theta}^2(x_i). \quad (14)$$

- **MC-Dropout Likelihood (MC NLL)**: We designed a method for combining MC-Dropout and ensemble in a single network. The NNs perform Monte-Carlo sampling before each back-propagation during the training phase. Similar to the ELL method above, we can calculate the mean and variance of the Monte-Carlo sample. Furthermore, injecting the mean and variance into negative log-likelihood (NLL) loss to perform back-propagation.
- **Deep Gaussian Processes (DGP)**: Deep Gaussian processes (DGPs) [7], a Bayesian inference method, are multi-layer generalizations of Gaussian processes(GPs), the data is modeled as the output

of a multivariate GP, where training and inference is performed using the method of [33] that can be used effectively on the large-scale data. We apply the DGP with two hidden layers and one output layer on all data-sets in our experiment.

- Isotonic regression (ISR): A simple non-parametric post-processing calibration method [19], which can recalibrate any regression algorithm similar to Platt scaling for classification. It is a separate auxiliary model to calibrate the probability output for a pre-train model and does not affect the original prediction of the model.

## B.2 Hyperparameters

Since the model structure is universal for all methods, we adjust the same optimal hyperparameters on the training data. Finally, we use the Adam [18] algorithm for the optimization with learning rate  $10^{-4}$  and weight decay  $10^{-3}$ . For the kernel function of MMD, we use a mixture of six RBF kernels  $k(x, x') = \sum_{i=1}^6 k_{\sigma_i}(x, x')$  with  $\sigma_i$  to be  $\{1, 4, 8, 16, 32, 64\}$  in all experiments. For data preprocessing, we scale the data into the range  $[0,1]$  to avoid extreme values and improve the computation stability.

## B.3 Datasets

- Bike Sharing <https://archive.ics.uci.edu/ml/datasets/bike+sharing+dataset>: This dataset contains the hourly and daily count of rental bikes between years 2011 and 2012 in Capital bikeshare system with the corresponding weather and seasonal information at Washington, D.C., USA.
- Uber-pickup <https://www.kaggle.com/yannisp/uber-pickups-enriched>: This is a forked subset of the Uber Pickups in New York City from 01/01/2015 to 30/06/2015 from Kaggle, enriched with weather, borough, and holidays information.
- PM2.5 <https://archive.ics.uci.edu/ml/datasets/Beijing+PM2.5+Data>: This hourly data set contains the PM2.5 data of US Embassy in Beijing, time period is between Jan 1st, 2010 to Dec 31st, 2014. Missing data are filled by linear interpolation.
- Metro-traffic <https://archive.ics.uci.edu/ml/datasets/Metro+Interstate+Traffic+Volum>: Metro Interstate traffic volume dataset, hourly Interstate 94 Westbound traffic volume for MN DoT ATR station 301, roughly midway between Minneapolis and St Paul, MN from 2012-2018. Hourly weather features and holidays included for impacts on traffic volume.
- Air-quality <https://archive.ics.uci.edu/ml/datasets/Air+Quality>: The dataset contains 9358 instances of hourly averaged responses from an array of 5 metal oxide chemical sensors embedded in an Air Quality Chemical Multisensor Device. The device was located on the field in a significantly polluted area, at road level, within an Italian city. Data were recorded from March 2004 to February 2005 (one year) representing the longest freely available recordings of on field deployed air quality chemical sensor devices responses.

Datasets	L	D	T
Uber-pickups	29102	11	1 hour
Bike-sharing	17389	16	1 hour
PM2.5	43824	13	1 hour
Metro-traffic	48204	9	1 hour
Air Quality	9358	15	1 hour
Power Plant	9568	4	nan
Protein Structure	45730	9	nan
Naval Propulsion	11934	16	nan
wine	4898	12	nan

Table 3: The description of dataset used, where L is length of time-series or data size, D is number of variables, T is time interval among series.

## C Metric Description

### C.1 The Metric of Prediction Precision

We also use RSE [20] and SMAPE [37] to quantify the prediction accuracy in addition to commonly used RMSE and  $R^2$  for time-series forecasting tasks. Root relative squared error (RSE), that can be regarded as RMSE divided by the standard deviation of test data. Compared to RMSE, RSE is more readable because it can ignore the influence of data scale and it is able to recognize outlier prediction results. So lower RSE value is better. Where  $y, \hat{y} \in \mathbb{R}^{n \times T}$  are ground truth and prediction value respectively.

$$RSE = \frac{\sqrt{\sum_{(i,t) \in \Omega_{\text{Test}}} (y_{it} - \hat{y}_{it})^2}}{\sqrt{\sum_{(i,t) \in \Omega_{\text{Test}}} (y_{it} - \mu(y))^2}} \quad (15)$$

Symmetric mean absolute percentage error (SMAPE or sMAPE) is an accuracy measure based on percentage errors. The absolute difference between  $y_i$  and  $\hat{y}_i$  is divided by half the sum of absolute values of the actual value  $A_t$  and the forecast value  $F_i$ . The value of this calculation is summed for every fitted point  $i$  and divided again by the number of fitted points  $n$ . Where  $y_i, \hat{y}_i$  are the ground truth and prediction value respectively.

$$\text{SMAPE} = \frac{100\%}{n} \sum_{i=1}^n \frac{|\hat{y}_i - y_i|}{(|y_i| + |\hat{y}_i|)/2} \quad (16)$$

### C.2 The Metric of Calibration

Different from quantifying calibration in classification tasks, such as Brier Score [5], Reliability Diagrams [9] and Expected Calibration Error (ECE) [28], the calibration error is usually quantified by prediction intervals for regression tasks. In order to quantitatively evaluate the accuracy of predictive uncertainty, we use the numerical score of calibration error as an metric similar to the diagnostic tool proposed by [19]. Because the probability value is less than 1, in order to better distinguish the performance of calibration, here we use the absolute distance between expected confidence and observed confidence different from [19].

**Calibration error.** We designed two metrics, ECPE and MCPE to quantitatively evaluate our experiments. The expectation of coverage probability error (ECPE) of prediction intervals (PIs) is the absolute difference between true confidence and empirical coverage probability. Relatively, the maximum value of coverage probability error (MCPE) of prediction intervals (PIs) is the maximum distance.

$$ECPE = \frac{1}{n} \sum_{j=1}^n |P_j - \hat{P}_j| \quad (17)$$

$$MCPE = \max |P_j - \hat{P}_j| \quad (18)$$

Where  $P_j$  is the expected confidence (i.e., the confidence level that we expect), and  $\hat{P}_j$  is probability that prediction intervals cover the ground truth.

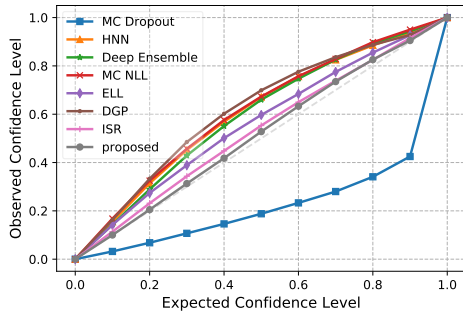
**Sharpness.** Another important aspect for evaluating calibration is the sharpness. We prefer prediction intervals as tight as possible while accurately covering the ground truth in regression tasks. We measure the sharpness using EPIW and MPIW. The expectation of prediction interval widths (EPIW) is averaged width of PIs, the maximum of prediction interval widths (MPIW) is the maximum width of PIs, reflecting the degree of uncertainty.

$$EPIW = \frac{1}{n} \sum_{j=1}^n \hat{Y}_{jup} - \hat{Y}_{jlow} \quad (19)$$

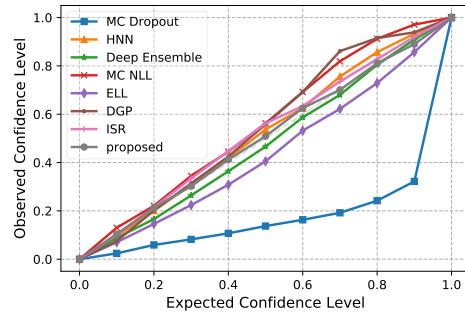
$$MPIW = \max(\hat{Y}_{jup} - \hat{Y}_{jlow}) \quad (20)$$

Where  $\hat{Y}_{jup}, \hat{Y}_{jlow}$  are the upper and lower bounds of prediction intervals respectively.

Figure 5 and 7 shows the proportion that PIs covering ground truths at different confidence levels. The result of our proposed model is most close to the diagonal line, which indicates the best uncertainty calibration among all methods. Figure 6 shows the predictions and corresponding 95% prediction intervals. The intervals are visually sharp and accurately cover the ground truths.

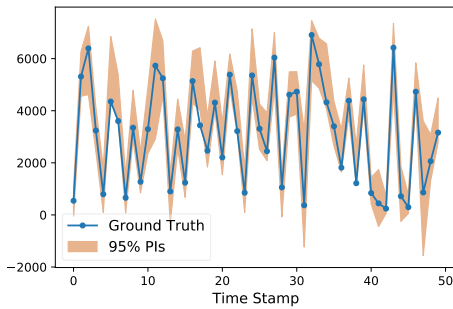


(a) Dataset: Metro Traffic.

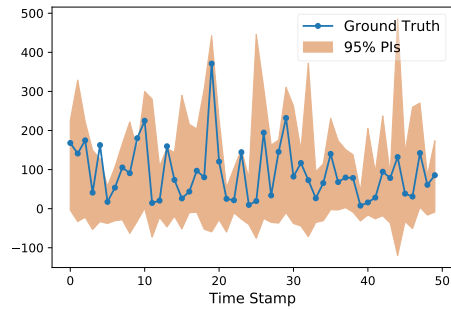


(b) Dataset: PM2.5.

Figure 5: Evaluating visually the quality of uncertainty by reliability diagrams. For each dataset, we plot the expected confidence vs observed confidence (empirical coverage probability) on the test data for compared baselines and proposed methods. It is obvious from the figure that observed confidence by our method is almost equal to the expected confidence.

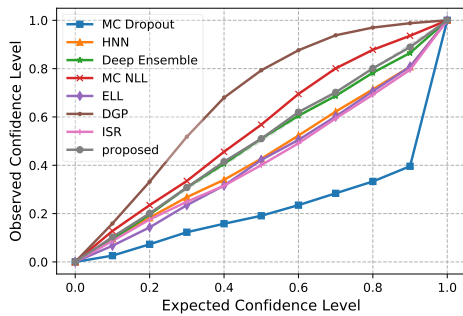


(a) Dataset: Metro Traffic.

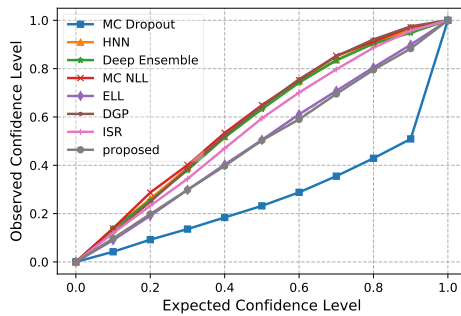


(b) Dataset: PM2.5.

Figure 6: Calibrated forecasting: Displayed prediction intervals (PIs) obtained at 95% confidence level by our proposed method in a time-series. As shown in the figure, the prediction intervals are also sharp while accurately covering the ground truth.



(a) Dataset: Wine.



(b) Dataset: Power Plant.

Figure 7: Evaluating visually the quality of uncertainty by reliability diagrams. For each dataset, we plot the expected confidence vs observed confidence (empirical coverage probability) on the test data for compared baselines and proposed methods. It is obvious from the figure that observed confidence by our method is almost equal to the expected confidence.

Dataset	Metric	HNN	Deep-ens	MC NLL	ELL	DGP	proposed
Metro-traffic	EPIW	786.42	788.03	1416.62	826.18	1155.69	<b>776.05</b>
	MPIW	2564.12	2569.37	4618.86	2693.74	3768.11	<b>2530.30</b>
Bike-sharing	EPIW	53.88	53.85	103.31	72.95	102.62	56.38
	MPIW	175.68	175.31	336.83	237.84	334.61	183.82
Pickups	EPIW	656.63	610.24	1748.87	827.60	847.00	625.57
	MPIW	2140.94	1989.67	5702.16	2698.37	2761.65	2039.67
PM2.5	EPIW	90.20	82.97	125.07	71.89	114.40	87.82
	MPIW	294.09	270.51	407.87	234.41	373.01	286.35
Air-quality	EPIW	108.50	105.59	143.43	105.60	145.98	<b>104.79</b>
	MPIW	353.77	344.27	467.66	347.77	475.95	<b>341.68</b>

Table 4: The calibration sharpness of uncertainty evaluation for each method on different datasets. Our method produces relatively sharp prediction intervals, note that the smaller width of the prediction interval is not better without the guarantee of smaller calibration error. We prefer the prediction interval as tight as possible while accurately covering the ground truth.

Dataset	Metric	MCD	HNN	Deep-ens	MC NLL	ELL	DGP	proposed
Metro-traffic	RMSE	523.6	556.3	508.9	631.6	613.5	646.4	545.5
	$R^2$	0.930	0.921	0.934	0.899	0.904	0.894	0.925
	SMAPE	15.76	15.68	14.90	21.21	18.41	20.82	17.47
	RSE	0.275	0.293	0.266	0.332	0.322	0.344	0.279
Bike-sharing	RMSE	38.86	40.71	37.60	89.57	52.50	55.39	37.93
	$R^2$	0.912	0.904	0.918	0.536	0.841	0.823	0.917
	SMAPE	36.54	31.98	27.25	63.96	35.59	45.94	29.38
	RSE	0.318	0.339	0.302	0.968	0.459	0.481	0.310
Pickups	RMSE	350.3	359.8	336.4	526.8	<b>325.9</b>	440.3	346.9
	$R^2$	0.967	0.965	0.969	0.925	<b>0.971</b>	0.944	0.967
	SMAPE	7.990	7.572	7.006	11.825	<b>6.824</b>	12.55	7.686
	RSE	0.189	0.194	0.181	0.295	<b>0.176</b>	0.249	0.185
PM2.5	RMSE	70.95	58.81	60.24	66.77	61.09	61.44	<b>57.43</b>
	$R^2$	0.154	0.264	0.389	0.250	0.372	0.365	0.298
	SMAPE	52.91	52.91	49.66	56.87	50.675	51.55	53.24
	RSE	1.111	1.083	1.290	1.930	1.254	1.469	<b>1.080</b>
Air-quality	RMSE	81.16	79.60	80.03	87.12	90.01	86.05	80.69
	$R^2$	0.829	0.836	0.834	0.804	0.790	0.808	0.832
	SMAPE	26.97	24.13	24.60	28.03	27.37	30.97	24.88
	RSE	0.451	0.451	0.454	0.511	0.535	0.483	0.456

Table 5: The prediction precision of each method on different datasets. We report the RMSE,  $R^2$ , SMAPE and RSE for each of the cases, each row has the results of a specific method in a particular metric. Our proposed method achieves competitive results in prediction precision, almost outperforming the results of HNN in all metrics.